Microelectronic Engineering 87 (2010) 1082–1085

Contents lists available at ScienceDirect

Microelectronic Engineering

journal homepage: www.elsevier.com/locate/mee

Modeling fluid velocity response for wafer scanning in immersion lithography

Hui Chen, Xin Fu, Jun Zou *, Huayong Yang, Xiaodong Ruan, Guofang Gong

The State Key Laboratory of Fluid Power Transmission and Control, Zhejiang University, Hangzhou 310027, China

ARTICLE INFO

Article history:
Received 10 September 2009
Received in revised form 12 November 2009
Accepted 12 November 2009
Available online 17 November 2009

Keywords:
Immersion lithography
Liquid renovation
Unsteady effect
Velocity distribution

ABSTRACT

In order to improve optical lithography resolution, a method has been proposed to insert a high refraction index liquid in the space between the lens and the wafer in place of the low refractive index air that currently fills the gap. During exposure period, the scanning process of wafer is repeated many times on a typical wafer, and the immersion liquid motion is greatly influenced by it. As a nominally scanning time of wafer is short (<0.1 s), the unsteady effect cannot be ignored, which play an important role in the immersion liquid renovation and optical birefringence. Considering the unsteady effect induced by the scanning process of wafer, models have been established to describe the limited flow field between the lens and the wafer.

1. Introduction

Immersion lithography has been accepted as a method for improving optical lithography resolution to 45 nm and below. The principle of immersion lithography is to increase the refraction index in the space between the final lens element and resist-coated wafer by insertion of a high refractive index liquid. Experiments have shown that Photo-Acid Generator (PAG) leaching from resist [1] and film peeling at the edge of wafer [2] can occur during immersion exposure. These phenomena will lead to the inevitable contamination of liquid which causes some problems, such as lens pollution [3] and watermark formation [4].

The liquid renovation is perhaps the best method to eliminate contaminations [5]. But it is greatly influenced by wafer motion due to the wall shear effect when the scanning velocity of the wafer is high. As a nominally scanning time of wafer is short (<0.1 s) and the scanning process is repeated many times on a typical wafer, the status of flow is changed quickly. The significant change of liquid renovation mainly occurs in the region near the wafer due to the wall shear effect, and it leads to the change of the whole flow velocity, especially when the direction of wafer scanning is opposite to the direction of flow driven by a liquid supply system. Moreover the shear stress of the increased viscosity of the liquid when compared with air results acting on the lens may cause the optical birefringence [6].

2. Physics of velocity response for wafer scanning

Liquid renovation is determined by the distribution of flow which is illustrated in Fig. 1, also can be written as [7]:

$$u(t,y) = u_n(t,y) + \frac{(P_{\text{in}} - P_{\text{out}})}{2\rho \nu L}(yh - y^2). \tag{1}$$

The velocity of the flow in the filled region $u(t,y)$ in Eq. (1) includes two terms. The first term $u_n(t,y)$ denotes the velocity driven by wafer motion. The other term represents the velocity due to the differential pressure driven by liquid supply system (Poiseuille flow). The parameters in Eq. (1) are shown in Table 1.

Keeping the liquid supply system unchanged, from the Eq. (1), it is easy to see that the effect of wafer motion is the key factor to achieve effective renovation of liquid. Considering the process of step-and-scan, the wafer velocity $U_n(t)$ varies as shown in Fig. 2. $U_n(t)$ increases form zero to the scanning velocity U_{scan} with an initial acceleration a_0. After being maintained for a certain time t_1, the velocity decreases at the opposite acceleration $-a$ until achieving the scanning velocity in the opposite direction $-U_{\text{scan}}$. This process is repeated nominally 71 times on a typical wafer [8].

We consider every wafer scanning or stepping is independent of each other. Assuming inertia-free, parallel flow and ignoring the influence of gravity, the equation for the flow velocity driven by wafer motion is

$$\frac{\partial u_n(t,y)}{\partial t} = \nu \frac{\partial^2 u_n(t,y)}{\partial y^2}, \quad y \in [0,h]. \tag{2}$$

The velocity of liquid on wafer is as same as the velocity of wafer, and the liquid velocity at the lens surface is zero. So the boundary conditions are

* Corresponding author.
E-mail address: junzou@zju.edu.cn (J. Zou).

0167-9317/$ - see front matter © 2009 Elsevier B.V. All rights reserved.
doi:10.1016/j.mee.2009.11.062

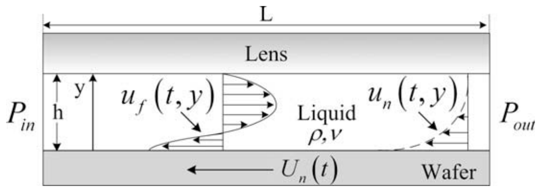

Fig. 1. Physical mechanisms that govern liquid renovation.

Table 1
Input parameters for immersion lithography anticipated operating conditions.

Parameter	Symbol	Value
Inlet pressure	P_{in}	100–1500 Pa
Outlet pressure	P_{out}	−1500 to −100 Pa
Density of liquid	ρ	1–2 g/cm^3
Viscosity of liquid	ν	10^{-7} to 10^{-3} m^2/s
Width of lens	L	30–70 mm
Lens-to-wafer height	h	0.1–2 mm
Scanning distance	d	25 mm
Scanning velocity	U_{scan}	0.25–0.75 m/s
Stepping acceleration	a_0, a	8 m/s^2

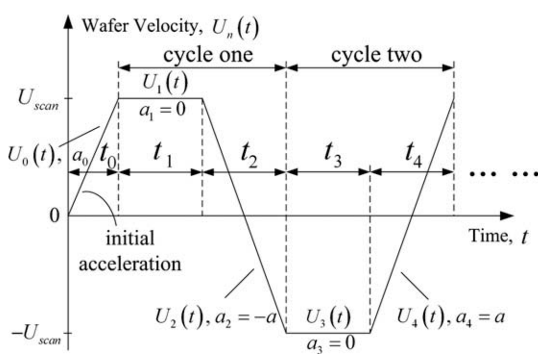

Fig. 2. Wafer velocity under oscillating conditions.

$$\begin{cases} u_n(t,0) = U_n(t), \\ u_n(t,h) = 0. \end{cases} \tag{3}$$

For the continuum of flow, the initial value of a wafer scanning or stepping can be calculated from the previous phase, therefore:

$$u_n(0,y) = \begin{cases} 0 & n = 0, \\ u_{n-1}(t_{n-1}, y) & n \geqslant 1, \end{cases} \tag{4}$$

where

$$t_{n-1} = \begin{cases} U_{scan}/a_0 & n = 1, \\ d/U_{scan} & n \text{ is even and } n > 1, \\ 2U_{scan}/a & n \text{ is odd and } n > 1. \end{cases} \tag{5}$$

Assume the flow velocity driven by wafer motion includes two terms, and it can be written as

$$u_n(t,y) = \frac{U_n(t)(h-y)}{h} + w_n(t,y), \tag{6}$$

where the first term represents the well-known Couette flow, and the second term $w_n(t,y)$ is the different value of velocity between the actual flow and the Couette flow. Substituting Eq. (6) into Eq. (2), we obtain:

$$\frac{\partial w_n(t,y)}{\partial t} = \nu \frac{\partial^2 w_n(t,y)}{\partial y^2} - \frac{\partial U_n(t)}{\partial t} \frac{(h-y)}{h}. \tag{7}$$

The initial-boundary-value problem becomes:

$$\begin{cases} w_n(t,0) = 0, \\ w_n(t,h) = 0, \end{cases} \tag{8}$$

and

$$w_n(0,y) = \begin{cases} 0 & n = 0, \\ u_{n-1}(t_{n-1}, y) - \frac{U_n(0)(h-y)}{h} & n \geqslant 1. \end{cases} \tag{9}$$

By the Eigenfunction Method [9], which is one of the classical methods of Partial Differential Equations. It is easy to get the exact solution of Eq. (7) with initial-boundary-value problem Eqs. (8), (9) as follows:

$$w_n(t,y) = \sum_{k=1}^{\infty} A_n(t,y), \tag{10}$$

where

$$A_n(t,y) = \frac{2a_n h^2}{k^3 \pi^3 \nu}\left(e^{\frac{-k^2\pi^2 \nu t}{h^2}} - 1\right)\sin\left(\frac{k\pi y}{h}\right) + A_{n-1}(t_{n-1}, y)e^{\frac{-k^2\pi^2 \nu t}{h^2}} \qquad n \geqslant 0, \tag{11}$$

and $A_{-1}(t_{-1},y) = 0$.

Evidently, the series (10) is convergent. The value of $A_n(t,y)$ decreases quickly as the increase of k, and the limitation of $A_n(t,y)$ is zero when k tends to infinity. So we can get the solution with high precision when the value of k is finite. In the following, we take $k = 500$.

3. Changing of maximum velocity driven by wafer motion

Form Eqs. (6)–(11), it is obvious to see the unsteady effect that the flow velocity $u_n(t,y)$ changes as scanning time t. The unsteady effect may lead to significant fluctuation of flow status, so it is important to understand the changing of maximum velocity of flow during wafer scanning.

Water has been used for 193-nm immersion, so we take it as immersion liquid to study the changing process of flow velocity considering the unsteady effect. We define the maximum velocity of flow during one scan cycle as the maximum velocity. The non-dimensional maximum velocity is given by

$$(\tilde{u}_n(t,y))_{max} = \frac{(u_n(t,y))_{max}}{U_{scan}}. \tag{12}$$

Without loss of generality, we estimate the variation of non-dimensional maximum velocity in center of flow ($y = h/2$) for 3 groups, respectively. It is shown in Fig. 3. The cycle time from −1 to 0 in Fig. 4 represents the process of initial acceleration of wafer as shown in Fig. 2. During this time, the speed of wafer is increased from zero to a given scanning speed. Then the wafer moves between scanning and stepping alternately. Closer examination of Fig. 3 reveals that the maximum velocity is stable for a given height of lens-to-wafer when the cycle time is lager than six. The instable process is just a small part of the whole process of step-and-scan. So it is appropriate to use the stable value to study the effect of wafer motion.

4. Liquid renovation for wafer scanning

We define the region where the stable value of non-dimensional maximum velocity is lager than 1/2 as the high-velocity region. It is easy to see that the significant change of flow status mainly occurs in the high-velocity region near the wafer due to the wall shear effect. Unfortunately the contaminations diffused from the wafer surface are mainly concentrated in this region.

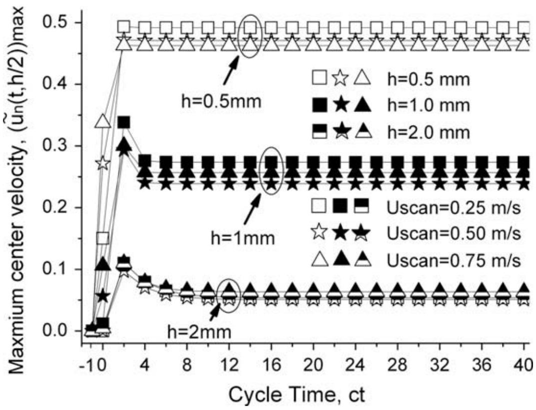

Fig. 3. Non-dimensionally maximum velocity in the center of lens-to-wafer for different scanning cycles.

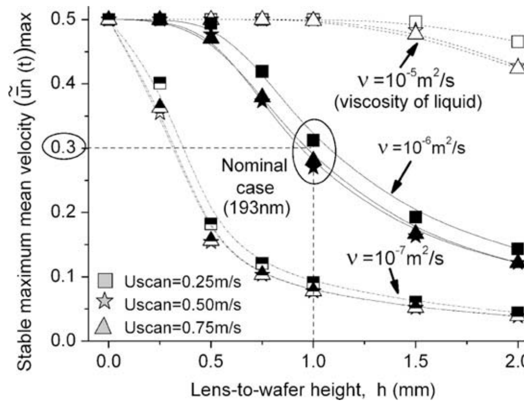

Fig. 5. Effect of the lens-to-wafer height and liquid viscosity on the non-dimensionally stable maximum mean velocity driven by wafer motion.

The flow velocity decreases gradually as the distance to wafer increases due to the wall shear effect, so we can get the critical position where the stable velocity is half of the wafer scanning velocity U_{scan}. The height of high-velocity region is the distance from the critical position to wafer. So the height of high-velocity region influences the extent of contamination, and it is necessary to get the height of this region to control the contaminations by optimizing the parameters of liquid supply system.

Fig. 4 shows the stable value of non-dimensional maximum for water as immersion liquid. It is easily seen that the height of high-velocity region is maintained at a certain value, and it is less affected by the lens-to-wafer height and the wafer scanning speed. Therefore, increasing the flow rate of external high-velocity region and the height of lens-to-wafer are two effective ways to inhibit the transport of contaminations to the under-lens region. It is worth noting that the height of high-velocity region is nearly 0.25 mm as the liquid is water and the lens-to-wafer height is larger than 0.5 mm. This means that the parameters of liquid supply system should be adjusted little for the different lens-to-wafer height.

When the direction of wafer scanning is opposite to the direction of flow driven by a liquid supply system, the minimum mean velocity of liquid supply system should be larger than the maximum mean velocity driven by wafer motion for effective liquid renovation. The non-dimensional maximum mean velocity is

$$\left(\tilde{\bar{u}}_{\mathrm{n}}(t)\right)_{\max} = \frac{\left(\int_0^h u_{\mathrm{n}}(t,y)dy\right)_{\max}}{h} \Big/ U_{\mathrm{scan}}. \tag{13}$$

The stable value of maximum mean velocity under different working conditions is shown in Fig. 5. For a given height and viscosity, there exists a constant ratio between the maximum mean velocity and wafer scanning speed. For the nominal case of 193-nm operating conditions, this constant value is nearly 0.3. For the effective liquid renovation, the minimum mean velocity driven by liquid supply system should be larger than 0.3 times of wafer scanning speed, unnecessarily greater than 0.5 times based on the assumption of the Couette flow.

5. Birefringence induced by shear stress

The flow of viscous immersion liquid leads to shear stress acted on the lens elements. It will induce birefringence, which can be estimated by [6]:

$$Bf = 2RC\tau_{\max}, \tag{14}$$

where R is lens thickness, C is the birefringence constant and $\tau_{\max}$ is the maximum shear stress. Assume the liquid is a Newtonian fluid, so $\tau_{\max}$ can be written as

$$\tau_{\max} = \mu \left| \frac{du_n(t,y)}{dy} \right|_{y=h} \Bigg|_{\max}, \tag{15}$$

where the dynamic viscosity μ is equal to kinematic viscosity v multiplied by density ρ. Assume lens thickness R is 50 mm, a birefringence constant C is 5 (nm/cm)/(kg/cm^2) and the wafer scanning speed is 0.75 m/s. For different height of lens-to-wafer and viscosity of liquid, the values of maximum birefringence during wafer scanning are shown in Fig. 6.

It is obvious that the birefringence can be neglected in most cases except for the case of high viscosity and low height of lens-to-wafer. For 157-nm immersion, perfluoropolyethers (PFPEs) are

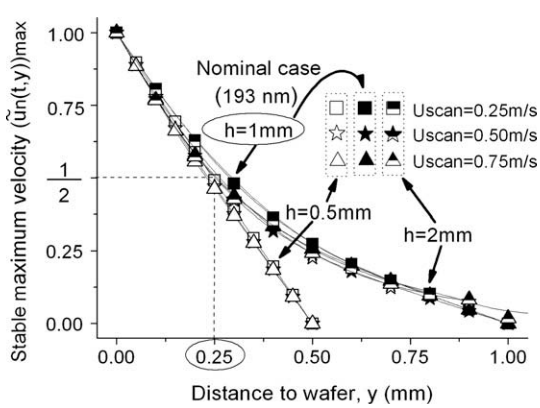

Fig. 4. Distance to wafer versus the non-dimensionally stable maximum velocity as the immersion liquid is water.

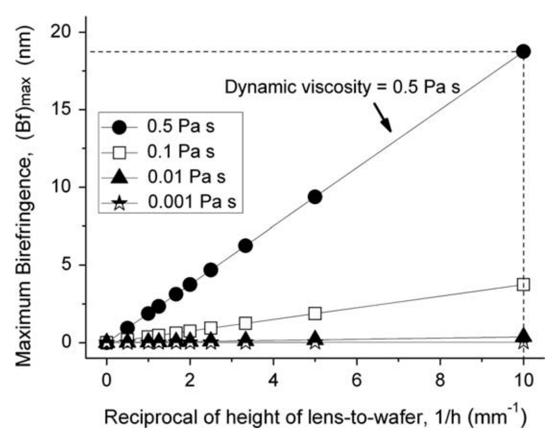

Fig. 6. The maximum birefringence as wafer moves at 0.75 m/s.

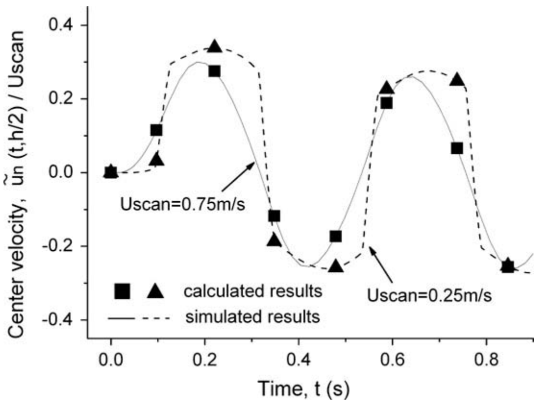

Fig. 7. Non-dimensionally velocity in the center of lens-to-wafer as wafer moves at 0.75 m/s.

assumed to be the immersion liquid. When the dynamic viscosity is 0.5 Pa s and the lens-to-wafer height is 0.1 mm, the value of birefringence is larger than 18 nm as the wafer scanning velocity is 0.75 m/s. A new immersion liquid with low viscosity is helpful to reduce the birefringence of 157-nm immersion lithography.

6. Simulation results and discussion

Two-dimensional (2-D) computational fluid dynamics (CFD) models of the flow velocity between the lens and wafer are developed by using the software Fluent. The periodic boundary conditions [10] in inlet and outlet are introduced to eliminate the Poiseuille flow driven by the differential pressure. The simulation ignores the influence of gravity, and it is conducted by laminar model with the parameters listed in Table 1.

The velocity in center position ($y = h/2$) is obtained from calculation by Eqs. (6)–(10) and simulation. As shown in Fig. 7, the case corresponding to the anticipated 193-nm operating conditions ($v = 10^{-6}$ m^2/s, $h = 1$ mm) is investigated as wafer moves at different velocities. It is clearly shown that the simulated results accord with the calculated results from the models considering the unsteady effect.

7. Conclusion

In this work, the analytical models considering the unsteady effect are applied to analyze the impact of wafer scanning on liquid renovation and the birefringence, and it is verified by simulation using CFD models. The results show that the flow is greatly impacted by viscosity of liquid v and the height of flow h. When the immersion liquid has low viscosity, there are significant differences between the flow considering unsteady effect and the Couette flow. At the anticipated 193-nm conditions, as long as the lens-to-wafer height is larger than 0.5 mm, the height of high-velocity region is nearly 0.25 mm. In addition, the minimum mean velocity driven by liquid supply system is just 0.6 times of the minimum mean velocity calculated by the Couette flow. So the parameters of liquid supply system can be simplified in a great extent. Moreover, the birefringence generated by wafer motion can be neglected except the flow with ultra-high viscosity and low height of lens-to-wafer.

Acknowledgements

The authors are grateful to the International S&T Cooperation Program of China (Grant No. 2008DFR70410), the Zhejiang Provincial Natural Science Foundation of China (Grant No. D1080038) and Key Industrial Program of Zhejiang Province of China (Grant No. 2008C11069).

Appendix A. Supplementary material

Supplementary data associated with this article can be found, in the online version, at doi:10.1016/j.mee.2009.11.062.

References

[1] S. Gaugiran, R. Feilleux, C. Sourd, S. Warrick, V. Farys, et al., Microelectron. Eng. 84 (2007) 1054–1057.
[2] M. Terai, T. Ishibashi, T. Hagiwara, T. Hanawa, et al., J. Photopolym. Sci. Technol. 21 (2008) 665–672.
[3] G.F. Nellis, M. Ei-Morsi, C. Van Peski, A. Grenville, J. Microlith. Microfab. Microsyst. 5 (2006) 013007.
[4] D. Kawamura, T. Takeishi, K. Sho, K. Matsunaga, N. Shibata, et al., Proc. SPIE 5753 (2005) 818–826.
[5] Wenyu Chen, Ying Chen, Jun Zou, Xin Fu, Huayong Yang, J. Vac. Sci. Technol. B 27 (2009) 2192–2199.
[6] A. Wei, A. Abdo, G. Nellis, R.L. Engelstad, et al., Microelectron. Eng. 73–74 (2004) 29–34.
[7] J. Fay, Introduction to Fluid Mechanics, MIT Press, Cambridge, MA, 1994.
[8] M. Ei-Morsi, G. Nellis, S. Schuetter, C. Van Peski, J. Vac. Sci. Technol. B 23 (2005) 2596–2600.
[9] Lawrence C. Evans, Partial Differential Equations, American Mathematical Society, 1998.
[10] FLUENT 6.3 User's Guide, ANSYS Inc., 2006.